

DYNAMICS OF PLASMA HEATING IN A STRAIGHT TURBULENT DISCHARGE

N. K. BERGER, V. S. KOĬDAN, A. N. POPYRIN, A. G. PONOMARENKO, V. N. STIBUNOV, and B. A. YABLOCHNIKOV

Nuclear Physics Institute, Siberian Branch, U.S.S.R. Academy of Sciences

Submitted December 6, 1968

Zh. Eksp. Teor. Fiz. 56, 1463-1479 (May, 1969)

We present the results of an investigation of plasma heating by a current in a straight discharge. The development of turbulence has been investigated by means of Langmuir probes, an electrostatic analyzer, and diamagnetic and x-ray transducers. It is shown that the appearance of an anomalous resistance and a rise in absorbed energy depend on the density and temperature of the initial plasma. A characteristic feature in the strong-turbulence stage is the fact that the total potential drop is concentrated in a specific region of the plasma, this region being characterized by the most intense rf oscillations. The maximum values of the anomalous resistance and the voltage across the discharge gap are observed at the time of a sharp reduction in current; at this same time there is observed a strong back current (electrons) to the cathode. The onset of turbulence is characterized by the expansion of the plasma to the walls of the chamber. Possible causes for the observed effects are discussed.

INTRODUCTION

At the present time a body of literature exists which is devoted to the experimental investigation of plasma heating in a straight turbulent discharge.^[1-6] New experiments have been reported very recently which indicate the possibility of heating plasma ions in discharges of this kind.^[7,8] In view of their importance for the problem of controlled thermonuclear fusion, undoubtedly these results will stimulate more detailed investigations of the heating mechanism and the physical nature of turbulence. These results also indicate the possibility of verification of some of the basic ideas in the theory of turbulent heating and the establishment of certain quantitative relations associated with collective effects in plasmas.^[9-12] The present work is devoted to a presentation of experimental results that have been obtained in an investigation of plasma heating by a current in a straight discharge and to some of the features of the dynamics of this process.

DESCRIPTION OF THE APPARATUS AND METHOD OF MEASUREMENT

A block diagram of the apparatus is shown in Fig. 1. A glass vacuum chamber is located in a quasistationary magnetic field $H_0 = 0-3$ kOe produced in a mirror device with a mirror ratio of 1:2. The electrodes are fabricated from stainless steel (ϕ 7 cm diameter) and can be moved freely along the axis of the tube in the region of uniform magnetic field. The experiment is carried out by using continuous injection of gas with preliminary ionization in a Penning discharge. By changing the chamber pressure and the discharge voltage it is possible to obtain a wide range of density and electron temperature in the initial discharge ($n_0 = 10^{11}-3 \times 10^{13}$ cm⁻³, $T_{e0} = 0-15$ eV). The values of n_0 and T_{e0} are measured with an 8-mm interferometer, by microwave measurements at a wavelength λ equal to 0.8 and 3 cm, and with Langmuir probes. The basic discharge is excited by switching a capacitor bank $C_0 = 0.2 \mu F$ charged

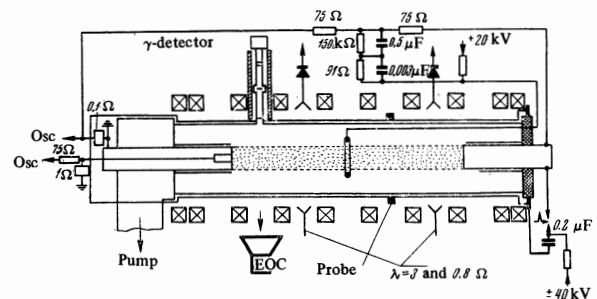


FIG. 1. Diagram of the apparatus.

to a voltage $\tilde{U}_0 = 0-40$ kV.

In choosing the diagnostic methods described below we have made use of the results of the theory of a turbulent discharge developed in [2,9,10]. The notion of an effective collision frequency ν_{eff} and effective resistance R_{eff} for the plasma discharge, as given in the theory, makes it possible to use macroscopic methods for measuring the electrical parameters which appear as variables in the equations that describe the flow of current and energy in the discharge circuit:

$$\tilde{U} = IR_{eff} + d(LI) / dt, \tag{1}$$

$$LI^2 + \int IV dt = C_0 U_0^2 / 2. \tag{2}$$

The discharge current I and the derivative of the current \dot{I} are measured respectively with a low-inductance shunt $r = 0.1 \Omega$ and a Rogowski loop. The voltage across the discharge gap is measured by means of a capacitive divider with a matched impedance in order to suppress parasitic oscillations. The quantities L and \dot{L} are measured by two mutually supporting methods: from Eq. (1), when $IR_{eff} \rightarrow 0$, which is a valid approach only in the second half-cycle of the discharge, and by direct measurement of the transverse dimensions of the plasma as seen with an electron-optical converter (electronic image converter).

In order to understand the mechanism by which turbulence is produced in the straight discharge it is nec-

essary to carry out a series of differential measurements. These include primarily measurements of the electric field in the plasma, measurements of the spectrum of excited oscillations, measurements of the distribution of electrons at the anode with respect to energy, and the determination of the transverse electron energy by means of x-ray detectors and diamagnetic probes.

The distribution of potential over the length of the plasma is measured by means of five Langmuir probes of coaxial construction and 0.4 cm diameter. In order to eliminate the inductive component the probes are located along the axis of the discharge toward the grounded electrode and are connected to a high-voltage capacitive divider with matched impedances.

The current density at the axis of the discharge and the energy distribution of the current-carrying electrons is measured by a three-grid electrostatic analyzer which is also located inside the grounded electrode. When the high-voltage electrode is maintained at a positive polarity it is possible to measure the ion component of the discharge current. The coaxial construction of the analyzer in conjunction with the small input aperture of 2 mm diameter and the pulsed application of a retarding potential to the grid provides a satisfactory sensitivity and resolution time 10^{-7} sec in the complete absence of internal breakdown.

The investigation of the oscillations that are excited in the passage of the current is carried out primarily in the region of the characteristic plasma frequencies ω_{0e} and ω_{0i} . The device used as a detector for the plasma radiation and the determination of the spectral composition of the radiation in the region of the electron plasma frequency makes use of waveguides beyond cutoff. The measurements at low frequencies $\omega \sim \omega_{0i}$ are carried out by means of resonance wave meters $\lambda = 3-100$ cm which are connected directly to the collector in the electrostatic analyzer. The spectrum of oscillations obtained in this way is then compared with the oscillations recorded by probes which measure the potential distribution in the plasma.

The transverse energy of the plasma is measured by two methods: x-ray transducers and diamagnetic probes. γ -photons with energies higher than 10 keV are measured by a single-channel stilbene spectrometer with 30 mm diameter and $d = 4$ cm thickness, which has a low scintillation time $t \sim 7 \times 10^{-9}$ sec and relatively high light output. The amplitude calibration of the spectrometer is carried out by means of an x-ray tube. The detection of soft x-ray radiation is carried out directly in the vacuum volume, also making use of scintillation methods. A thin plastic scintillator with 3.3 cm diameter and thickness $d = 0.5$ mm is shielded against visible radiation by a carbon layer $d \approx 0.0012$ g/cm² and is fastened by OK-50 compound to a light pipe which is connected to an FEU-53 photomultiplier. In front of the scintillator there are aluminum, copper or polyethylene absorbers of different thicknesses. A similar transducer is located on the opposite side of the discharge chamber and is used to monitor the measurements.

The diamagnetic probe is a carefully shielded coil made up of two turns mounted on the outer surface of the chamber in the region of the uniform magnetic field (cf. Fig. 1). The value of the electron density (averaged

over the diameter) and the transverse dimensions of the plasma at the location of the diamagnetic probe are determined by microwave probing at three wavelengths 3, 0.8 and 0.4 cm, and by streak photography using a transverse slit in conjunction with the image converter. Most of the measurements are carried out with air, in which case the discharge electrodes are located in the region of uniform magnetic field of the mirror device.

EXPERIMENTAL RESULTS

It was evident from the first experiments that the energy absorbed in the plasma, the volt-ampere characteristics, the real resistance of the discharge, the potential drop across the column, and the low-frequency and high-frequency oscillations, were sensitive to the parameters of the initial plasma and determined, as a rule by the ratio $\eta \approx j_{\sim}/j_0$ where $j_0 \approx en_0v_0$, $v_0 = \sqrt{2kT_e/m}$ and n_0 are the thermal velocity and density of the electrons in the initial plasma while the quantity $j_{\sim} = I/S$ is bounded from above by the values of the circuit parameters: $j_{\sim} = \tilde{U}/\rho S$; here, $\rho = \sqrt{L/C_0}$ is the characteristic resistance while S is the cross section through which the current flows; in the initial stage this cross section depends on the skin depth.

In Fig. 2 we show the results of measurements of the electron density in the initial plasma carried out by the

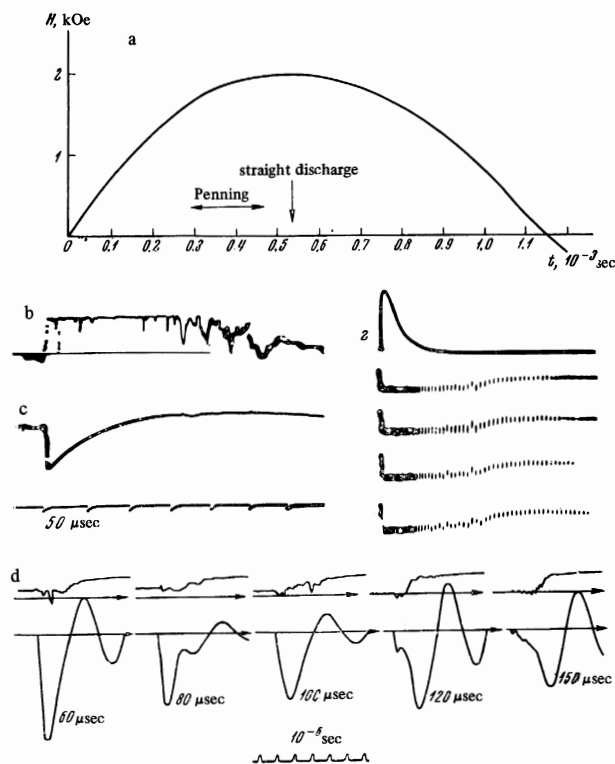


FIG. 2. Determination of the parameters in the initial plasma. a) quasistationary magnetic field H_0 ; the arrows indicate the time at which the initial and main discharges are switched on. b) microwave signals $\lambda = 3$ cm. c) Penning current, $I \sim 100$ A, d) microwave signal obtained with the 0.8 cm interferometer with time markers at approximately 5 μ sec. e) the current shape and the energy absorption in the straight discharge as functions of the density of the initial plasma. $I \approx$ kA when $t = 80$ μ sec. The upper trace shows the microwave signal at $\lambda = 0.8$ cm.

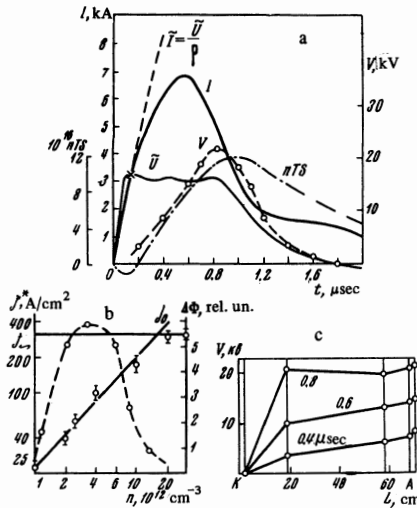


FIG. 3. Dynamic characteristics of a straight discharge. a) I discharge current; \tilde{U} and V are respectively the total and real voltage across a column; nTS is the diamagnetic signal; $\tilde{U}_0 = 30$ kV; $H_0 = 1.8$ kOe; $n_0 = 2 \times 10^{12}$ cm $^{-3}$; the operating gas is air; $p_0 = 5 \times 10^{-5}$ mm Hg. b) the critical current density j^* (solid curve) and the diamagnetic signal $\Delta\Phi$ (dashed curve) as functions of the density of the initial plasma n_0 . c) potential distribution over the length of the discharge at various times following the initiation of the discharge; K)cathode, A)anode.

8-mm interferometer and by microwave probing at wavelengths of 0.8 and 3 cm. The shape of the current pulse in the discharge depends on the delay with which it is fired with respect to the Penning discharge. At small delay times ($\eta < 1$) the current shape is approximately sinusoidal with small absorption, whereas at large values ($\eta > 1$) the rise of the current is significantly retarded and has a clearly-defined aperiodic nature in the first half-cycle (cf. Fig. 2d).

In Fig. 3a we show the typical dependence on time of the basic parameters that characterize the onset of the turbulent state in the discharge. At the beginning, before reaching $\eta \approx 1$ (in Fig. 3a this time is denoted by the cross) the current in the plasma is determined by the characteristic resistance; then, when $\eta > 1$, a rise is extended, indicating the appearance of additional resistance in the circuit. The fact that the resistance is real is verified by the corresponding increase in the real voltage drop V across the column and the effective absorption of energy in the plasma, as can be seen from the diamagnetic signal.

The condition for the onset of turbulence $\eta \gtrsim 1$ is verified experimentally in the following way. For a fixed value of $C_0 = 0.2$ μ F and voltage $\tilde{U}_0 = 30$ kV the mode of operation of the initial discharge can be varied over a wide range of electron density $n_0 \approx 5 \times 10^{11} - 2 \times 10^{13}$ cm $^{-3}$ and, by appropriate choice of the delay in triggering the main discharge, it is possible to maintain a fixed value of the electron temperature $T_{e0} \approx 5$ eV. The latter feature is provided by the linear dependence $j_0 \approx en_0 v_0$ on electron density in the initial plasma. In Fig. 3b we show the experimental values for the critical current density $j^* = I^*/S$ starting at which the turbulence regime appears in the discharge. There is a particularly good agreement between the onset of turbulence and the condition $\eta \gtrsim 1$

over the entire range of variation of n_0 . Because of the rather complex nature of Fig. 3a we have not shown the time behavior of the absorption of energy in the plasma $W(t)$; however, knowing the functions $V(t)$ and $I(t)$ we can easily establish that the largest value of $W(t)$ is achieved at approximately the time of maximum real voltage across the discharge. At approximately the same time there is also observed a peak in the diamagnetic signal $\Delta\Phi \sim n(T_e + T_i)S$. A detailed analysis of the oscillograms of $V(t)$ and $I(t)$ shows that the total energy evolved in the current flow

$$W(t) = \int_0^t I(t)V(t)dt,$$

is a sensitive function of the quantity η . It reaches some optimum value when $\eta \gtrsim 3$ and then falls off slowly when η is increased further. The effect of the parameter η on the quantity W can be easily understood if account is taken of the fact that at the point of maximum energy absorption the effective resistance of the plasma R_{eff} is approximately the same as the characteristic impedance; when $\eta \gg 1$ we find $R_{\text{eff}} \gg \rho$ and when $\eta \lesssim 1$ we find $R_{\text{eff}} \ll \rho$ (cf. Fig. 2d). The dependence of the diamagnetic signal $\Delta\Phi$ (transverse energy of the plasma particles) on the parameter η is similar to the functional dependence $W(\eta)$ only in the range $\eta = 1-5$; When $\eta > 5$ these quantities start to exhibit different behavior. It is evident from Fig. 3b that when $\eta > 5$ the quantity $\Delta\Phi$ falls off rapidly.

We start our analysis with the most interesting case, in which $\eta \approx 3-5$. In Fig. 3c we show the results of measurements of the potential distribution along the axis of the discharge at different times. It will be evident that the real voltage that appears across the column tends to be concentrated in a certain region, the region near the cathode. The electric field at the cathode reaches values of $E \approx 10^3$ V/cm whereas the remaining portion of the column exhibits values that vary over the range $E = 0-100$ V/cm; when $t \approx 0.8 \times 10^{-6}$ sec the voltage can even be in the opposite direction. Starting from the equation

$$\frac{ne^2}{m} E(z) + \frac{e}{m} \nabla p_e = j_{\text{veff}},$$

the origin of the formation of a potential well 2-3 kV appears to be indicated in the term that depends on the gradient of the electron pressure. That is to say, if it is assumed that the electrons that leave the cathode can transfer a significant fraction of their directed energy to cold electrons in the plasma in a distance of 10 cm, then over the remainder of the column the discharge current is maintained by virtue of thermal diffusion of electrons in the direction of the anode.

In Fig. 4 we show four different oscillograms obtained with approximately the same parameters of the initial plasma: $n_0 \approx 2 \times 10^{12}$ cm $^{-3}$, $T_{e0} \approx 5$ eV and $H_0 \approx 1.5$ kOe. We also show the corresponding distributions of the real voltage over the length of the plasma plotted for the time at which the quantity V reaches its peak value. The following conclusions can be drawn from this data: given approximately the same initial conditions (n_0, T_{e0}) the region of the principal real voltage drop can be displaced along the axis of the discharge and has a rather finite localization of approxi-

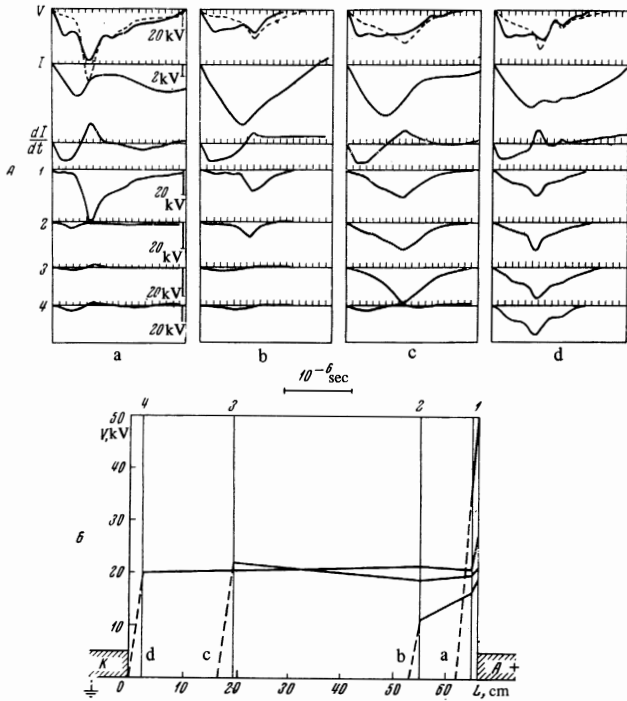


FIG. 4. Experimental data showing the local voltage drop in the discharge gap. A) oscillograms of the voltage V . (solid line—hollow, dashed line—real voltage across the column), the current I (in kA), the derivative of the current dI/dt ; 1, 2, 3, 4) signals from the probes that measure the potential at various points in the plasma as indicated on the lower portion of the figure. B) potential distribution for various current shapes (a, b, c, d); operating conditions $\bar{U}_0 = 30$ kV, $n_0 \approx 2 \times 10^{12}$ cm $^{-3}$, $H_0 \approx 1.5$ kOe, air.

mately 5 cm; this was determined experimentally by special measurements using probes located close together. This result means that it is at precisely this point that the primary energy of the current must be evolved and it is this section that exhibits the anomalously high real resistance R_{eff} .

A more detailed time pattern of the onset of turbulence can be seen in Fig. 5. The magnitude of the current in the initial stage is determined primarily by the resistance $\rho = \sqrt{L/C_0}$ and then, at some time t_1 , a real resistance arises in the circuit R_{eff} ; this resistance rises rapidly to a value that exceeds ρ by approximately an order of magnitude. Starting at time t_2 the quantity R_{eff} although diminishing, still maintains a high value for a relatively long time. On the current oscillogram one observes in this regime a characteristic plateau or dip. The duration of the dip, as has been established by means of a time-sweep investigation of the emission from the transverse dimension of the plasma, is a sensitive function of the time at which hot plasma is lost to the chamber walls. The sweep rate of the vertical slit obtained by means of the image converter (Fig. 6) shows that at the onset of the instability the plasma starts to expand with a velocity $v_{\perp} \approx \sqrt{kT_{e\perp}/M}$ while the microwave probe signals indicate a reduction in the electron density. Simultaneously, measurements of the electron density during current flow and pictures taken with the image converter show that the motion of the emitting boundaries toward the walls of the chamber is

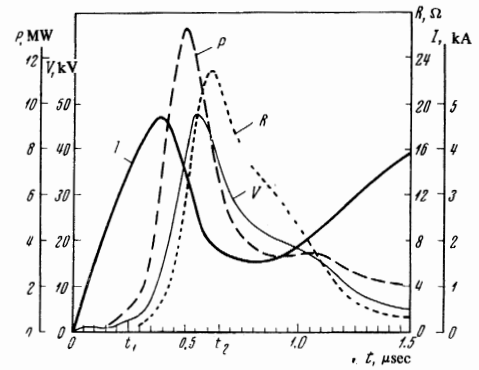


FIG. 5. Oscillograms of the current I and the real voltage V ; P) power, R) real resistance of the discharge gap. Operating conditions: $\bar{U}_0 = 30$ keV, $n_0 \approx 2 \times 10^{12}$ cm $^{-3}$, $H_0 = 1.5$ kOe, air.

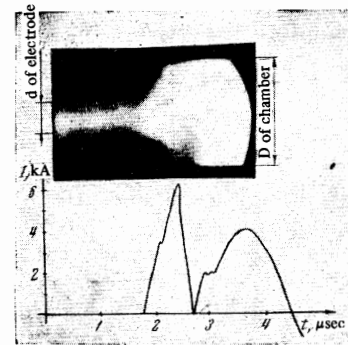


FIG. 6. Streak photograph of the emission from the transverse dimension of the plasma with turbulent heating. $\bar{U}_0 = 30$ kV, $n_0 = 2 \times 10^{12}$ cm $^{-3}$, $H_0 = 1.5$ kOe. The lower trace shows the current in the straight discharge.

evidently of a diffusion nature since the observed reduction in density (a factor of 2 or 3) does not correspond to an increase in the transverse cross section of the plasma by approximately a factor of 5–7. At the same time, the value $\beta = nT_{\perp}(H^2/8\pi) \ll 1$, observed in other experiments, verifies the assumption given above. In Fig. 6 we can see the clearly defined motion of the emitting boundaries of the plasma and the subsequent rather sharp drop of current. At this point a rather high real voltage exists across the gap.

The oscillograms of the signal from the collector of the electrostatic analyzer (Fig. 7) show that at the time the current drops, and even somewhat earlier, there is a motion of electrons against the electric field toward the cathode of the discharge. It will be evident from Fig. 7 that at first the collector signal is negative, corresponding to ion current (the analyzer is located at the cathode); then, starting with the onset of turbulence, the signal becomes positive (electrons!), reaching a peak at the time of the sharp reduction in the main discharge current. The energy analysis carried for the electrons moving against the field shows that they have a distribution which is approximately Maxwellian with a mean energy of 0.1 eV, which is of the order of the real potential drop in the plasma at that time. In certain cases the back current density of the electrons is comparable with

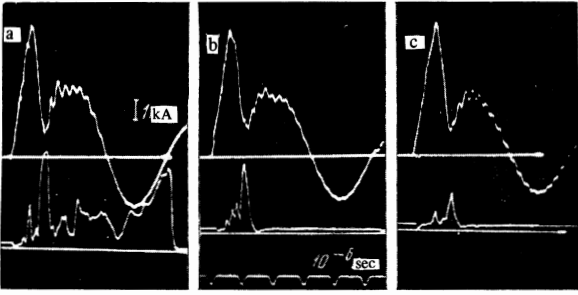


FIG. 7. Current due to electron motion against the electric field toward the cathode. The upper oscillogram shows the discharge current while the lower oscillogram shows the current at the collector or the analyzer. The retarding potentials are as follows: a) $U_R = 0$; b) $U_R = 500$ V; c) $U_R = 1200$ V. Operating conditions $\bar{U}_0 = 20$ kV, $n_0 = 2 \times 10^{12} \text{cm}^{-3}$, $H_0 = 1$ kOe, air.

the density of the forward current (in Fig. 7 $j_{\text{back}} \approx 0.65 j_{\text{for}}$). Under these conditions the discharge is extinguished in a short time.

Thus, it would appear that the state with the relatively long-lived large real resistance is characterized by motion of some hot electrons across the discharge and along the discharge in the opposite direction to the electric field (at the time of a sharp current drop).

Further experiments have shown that the loss of electrons to the walls of the chamber leads to outgassing and the development of another breakdown, which tends to shunt the large real resistance characteristic of the turbulent evolution of energy in the plasma. Microwave measurements at a wavelength of 0.4 cm show that after the secondary breakdown a plasma is formed with a density that exceeds the initial density by two orders of magnitude ($p_0 \approx 8 \times 10^{-5}$ mm Hg, $n_0 \approx 2 \times 10^{12} \text{cm}^{-3}$ while $n_{\text{final}} \gtrsim 7 \times 10^{13} \text{cm}^{-3}$). As is evident from Fig. 4, the break in the current described above is not always a sharp one as in an oscillogram such as a. However, it is specifically in this case that one observes the best defined basic features of the development of the instability in the turbulent discharge.

The dynamics of the heating of the plasma as a result of the development of the instability are illustrated vividly by measurements of the energy distribution of the current-carrying electrons that appear at the anode. In Fig. 8 we show oscillograms of the discharge current and the electron current at the collector of the analyzer for various values of the retarding potential. Satisfactory reproduction of experimental results is obtained when the capacity C_0 is charged to a voltage of the order of 10 kV; hence the most careful measurements are carried out in this range of operating values of \bar{U}_0 . An analysis of the oscillograms and semilogarithmic plots of the curves for the distribution $j_a(U_R)$, where U_R is the retarding potential in the grid analyzer, indicate that the electron spectrum is essentially Maxwellian while the discharge current at the anode is determined by the random electron current $j_a = (1/4)envT_e$, where $vT_e \approx \sqrt{2kT_{\parallel}/m}$. Using the analyzer to measure the quantity j_a and determining $T_{e\parallel}$ from the slope of the semilogarithmic characteristic we have found it possible to estimate the hot-electron density. For the two times corresponding to the maximum discharge current and the maximum energy ab-

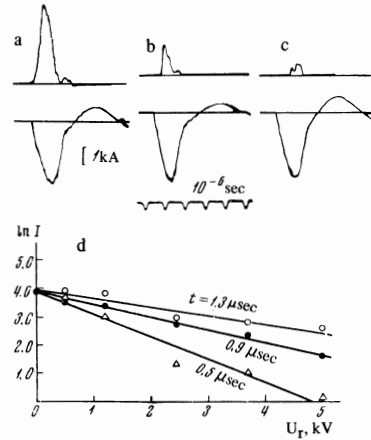


FIG. 8. The current at the collector of the analyzer as a function of retarding potential. $\bar{U}_0 = 10$ kV, $n_0 = 2 \times 10^{12} \text{cm}^{-3}$, $H_0 = 1$ kOe and the working gas is air. a) $U_R = 0$, j of the discharge is 90 A/cm^2 , j in the collector is 140 A/cm^2 ; b) $U_R = 2.4$ kV; c) $U_R = 5$ kV; d) curves showing the electron energy distribution for electrons striking the anode at different times.

sorption in the discharge we obtain the following data:

$$\begin{aligned} t_1 &= 0.9 \mu\text{sec}, & T_e &\approx 2.1 \text{ keV}, \\ & & n &\approx 1.4 \cdot 10^{12} \text{ cm}^{-3}; \\ t_2 &= 1.3 \mu\text{sec}, & T_e &\approx 3.0 \text{ keV}, \\ & & n &\approx 5 \cdot 10^{11} \text{ cm}^{-3}. \end{aligned}$$

Thus the magnitude of the current flow and the magnitude of the real voltage across the plasma increase together with $T_{e\parallel}$, the latter reaching a maximum value at the point of peak energy absorption in the discharge. The density of hot electrons is found to be very close to the density of the initial plasma and the reduction of the former at maximum heating is evidently associated with the expansion of the plasma. It is interesting to note that the measurement of the current density at this point indicates a compression of the current-carrying channel toward the axis of the discharge (in Fig. 8 the mean current density of the discharge is approximately 90 A/cm^2 whereas the density at the axis of the discharge is approximately 140 A/cm^2).

We now wish to consider the measurements of the transverse electron energy in the plasma. In Fig. 9 we show oscillograms that illustrate the rather good time

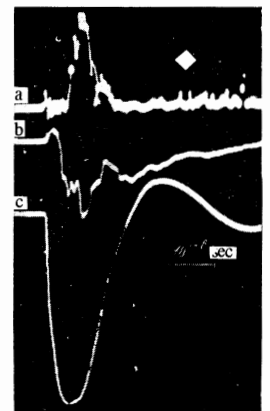


FIG. 9. Measurements of the transverse energy of the plasma in the turbulent regime. a) signal from the x-ray pickup; b) diamagnetic signal. $\Delta\Phi_{\text{max}} \sim 10^{17} \text{ eV/cm}^3 \cdot \text{cm}^2$; c) the discharge current $I_{\text{max}} \sim 7$ kA. $\bar{U}_0 = 30$ kV, $n_0 = 2 \times 10^{12} \text{cm}^{-3}$, $H_0 = 1.8$ kOe, air. $P_0 = 5 \times 10^{-5}$ mm Hg.

correlation between the signal from the soft x-ray transducer and the readings of the diamagnetic probe. The sharper rise in the increase of γ -radiation is explained by the fact that the polyethylene foils used for measuring the energy of the γ -photons set a limit on the initial level of detection to values of 300–500 eV. The same limitation holds for the decay of the signal from the x-ray transducer. As far as the absolute values found by the two methods are concerned we find that these give approximately the same value $T_{e\perp} \approx 1\text{--}2$ keV when $\bar{U}_0 = 30$ kV. It should be noted that in the analysis of the signal from the diamagnetic probe it is necessary to take account of the change in the electron density due to current flow as well as the expansion of the plasma.

Measurements of the hard x-ray radiation have shown that the strongest source of γ -photons is the anode of the discharge. The time at which the radiation appears coincides with the time of maximum real voltage across the column. In Fig. 10 we show a photograph of the anode as

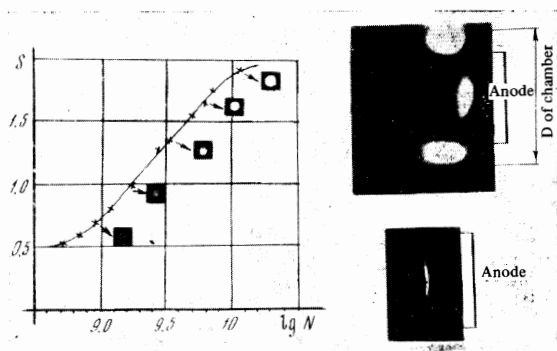


FIG. 10. Photographs of the anode in x-ray emission. S) relative degree of blackening; N) number of γ -photons with energies 15–20 keV per unit solid angle; $N_0 = N\Omega$; $\Omega = 2 \times 10^3$; $\bar{U}_0 = 30$ kV; $H_0 = 2$ kV, $n_0 = 2 \times 10^{12}$ cm $^{-3}$. The upper picture shows the anode in the mirror while the lower picture shows the anode in the region of uniform magnetic field.

obtained with an x-ray electron optical converter and a camera obscura. The electron optical converter is calibrated by means of an x-ray tube thus making it possible to determine the number of γ -photons with mean energy of approximately 20 keV. From a simple estimate $E_{\text{mean}}N_0 = \alpha cIV\Delta t$, where N_0 is the number of γ -photons determined in the experiment, α is the efficiency of the x-ray tube and c is the fraction of γ -photons with energies 15–25 keV we can obtain the mean current of electrons with energies of approximately 20 keV, which is found to be 300 A; this value corresponds to approximately 1/20 of the total current. Comparing the density of plasma and the density of fast electrons responsible for the hard radiation in the energy range 15–20 keV we see that the latter amount to 5% of the total electron density in the plasma. If the anode of the discharge is located in the region of the mirror, the γ -spectrometer records the hard radiation from the central region of the mirror machine. Evidently, as a result of the instability, some fraction of the fast electrons do not reach the anode and are trapped in the mirror (cf. Fig. 10). An estimate of the number of such electrons, carried out after the calibration of the γ -spectrometer, yields

a value of 5–10% with respect to the total number of particles in the plasma.

Results of measurements of the spectral composition of the oscillations produced by the current flow are shown in Fig. 11. In the onset of the turbulent state in the discharge we first find that microwave oscillations are excited at the electron-plasma frequency; then, after some delay, oscillations appear in the electron current at the collector of the analyzer. In Fig. 10 we show the spectrum of low-frequency oscillations which modulate the discharge current plotted taking account of the calibration of the detection system. It will be evident that at first the oscillations are concentrated in a narrow frequency region 200–300 MHz; then, as the amplitude increases this peak gradually becomes a distribution over the entire spectrum from 200 to 600 MHz, probably extending to still lower frequencies. In order to verify the hypothesis that current flow leads to the excitation of the ion-acoustic instability control experiments were carried out with different gases: air, helium, and xenon. The results of these experiments show that there is essentially no dependence of the frequency of the observed low-frequency oscillations on ion mass. The variable component of the potential at various points of the plasma exhibits a peak in the region of the potential well ($\Delta V \approx 1$ kV, $f \approx 200$ MHz) and its behavior with the flow of current is correlated with the observed drop of the low-frequency oscillations of the current-carrying electrons. In observing the high-frequency oscillations it is also necessary to take account of the fact that the intensity distribution over length is non-uniform and is localized in the region of the main potential drop. This feature was first observed by Lin and Skoryupin.^[13]

We now wish to consider the experimental results when $\eta \gg 1$. Under these conditions we find that a steady-state turbulent regime is established in time $t \sim 0.1$ μ sec. In Fig. 12 we show oscillograms by means of which it is possible to follow in detail the excitation of the instability which leads to the anomalous resistance and the absorption of energy in the plasma. A feature of

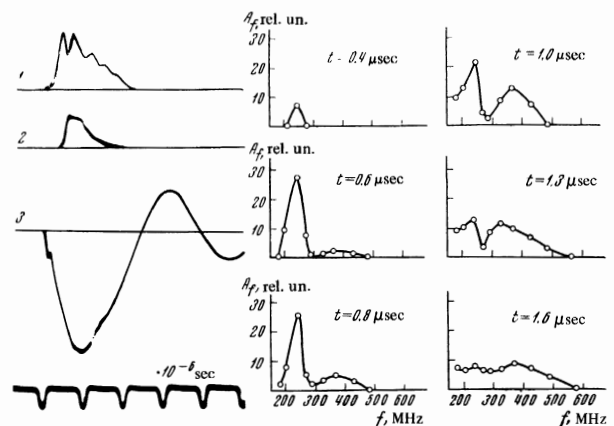


FIG. 11. Low-frequency oscillations of the current in the straight discharge: 1) current to the collector of the analyzer, 2) alternating component of the current at the collector $f = 200$ MHz, 3) discharge current $I_{\text{max}} = 7.5$ kA, $\bar{U}_0 = 30$ kV, $n_0 = 4 \times 10^{12}$ cm $^{-3}$, air at $P_0 = 8 \times 10^{-5}$ mm Hg. The figures to the right show the oscillation spectra at different times.

this regime is the fact that the effective resistance R_{eff} exhibits its largest value at the initiation of current flow, this value being $\sim 20 \Omega$; subsequently the resistance falls

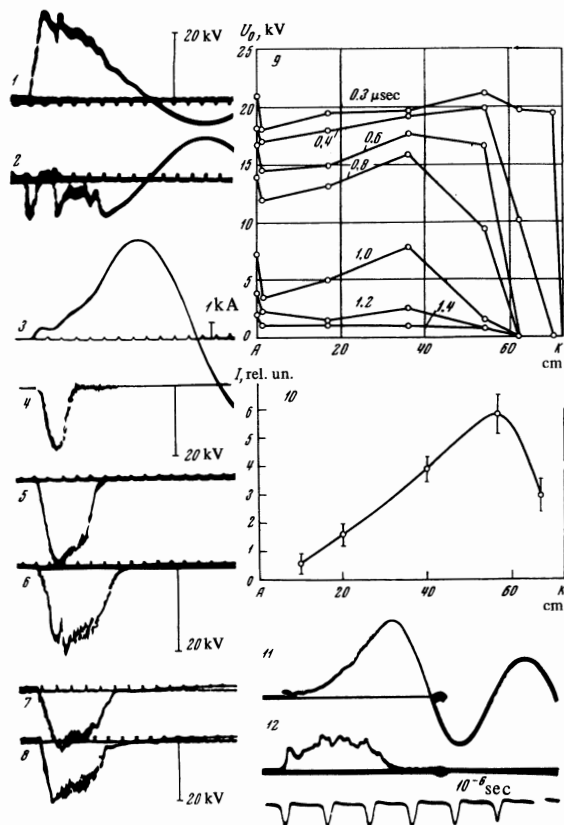


FIG. 12. Volt-ampere characteristics in the turbulent regime $n \gg 1$. 1) \bar{U} is the total voltage across the discharge gap; 2) dI/dt ; 3) is the discharge current; 4)–8) are signals from probes that measure the potential distribution along the column and probes located at the cathode and anode (the time markers on oscillograms 1 to 8 are $0.2 \mu\text{sec}$); 9) potential distribution over the length of the tube at different times; 10) distribution of the intensity of the radiation at the electron plasma frequency ω_{Oe} along the axis of the discharge; 11, 12) discharge current and microwave radiation at frequencies $\sim \omega_{\text{Oe}}$. $U_0 = 25 \text{ kV}$, $n_0 = 10^{12} \text{ cm}^{-3}$, $H_0 = 1.5 \text{ kOe}$, air.

off monotonically and this explains the clearly defined aperiodic nature of the discharge current. During this entire time the microwave detectors detect the presence of oscillations at the electron-plasma frequency with the greatest amplitude coming from the region containing the main potential drop. Sweep of the emission from the transverse slit with the image converter shows that at the beginning of the instability the plasma tends to emit uniformly over the entire chamber diameter. Analysis of the electrons arriving at the anode shows that the first electrons that leave the cathode experience substantial retardation. However, the energy distribution of these electrons differs from a Maxwellian one by the appearance of a rather well extended high-energy tail (cf. Fig. 13). Under these conditions it is difficult to establish a most probable velocity for the electrons arriving at the anode of the discharge. The diamagnetic mea-

surements show that the transverse pressure nT_{\perp} is $5-8 \times 10^{14} \text{ eV/cm}^3$ in the case $\eta \gg 1$ while the x-ray measurements give a value of $3-5 \text{ keV}$ for $T_{e\perp}$ which is close to the depth of the potential well (cf. Fig. 12). Using these data we find that the number of hot particles is $n \approx 10^{11} \text{ cm}^{-3}$, representing approximately 10% of the total number of electrons in the plasma. The observed incomplete relaxation of the first peak and the corresponding weakening of the diamagnetism are experimental results which have not as yet been explained uniquely.

DISCUSSION AND CONCLUSIONS

The experimental results presented here can be interpreted in the following way: a) the efficiency of plasma heating by the current in a straight discharge is a sensitive function of the parameters of the initial plasma; b) at a certain critical value of the current I a turbulent regime appears in the discharge, characteristic features being the anomalous resistance R_{eff} and plasma heating; c) there exists a limited region of the plasma (approximately 5 cm) in which the instability develops, this instability leading to the anomalous increase in resistance at this location; d) the absorption of energy in the plasma is also localized and increases in synchronism with the increase in R_{eff} and the real potential drop; e) the location of the largest potential drop in the discharge can be displaced along the plasma column as is indicated by the oscillogram in Fig. 4; f) for the largest break in the current a characteristic feature is the tendency for the region of anomalous resistance to concentrate at the anode of the discharge.

With the onset of the turbulent state in the plasma we find excitation of oscillations with frequencies $\omega \sim \omega_{\text{Oe}}$; these evidently determine the magnitude of the effective resistance $R_{\text{eff}} \approx m\nu_{\text{eff}}l/ne^2S$. If the quantity ν_{eff} is estimated from this relation it is found to lie within the limits $5 \times 10^8 - 3 \times 10^9 \text{ sec}^{-1}$ at various stages of the instability, in good agreement with the observed low-frequency oscillation spectrum and the dependence of the latter on time.

In accordance with the theoretical ideas developed, in particular, by Sagdeev^[9] and by Rudakov and Korabely,^[10] when a large current flows through a plasma a number of instabilities can be excited. For example,

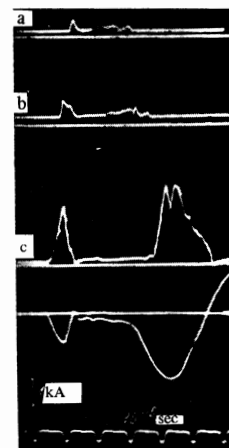


FIG. 13. The electron current at the collector of the analyzer as a function of retarding potential for $\eta \gg 1$. a) $U_r = 7.5 \text{ kV}$, b) $U_r = 3.5 \text{ kV}$, c) $U_r = 0$. The lower trace is the discharge current; $\bar{U}_0 = 10 \text{ keV}$, $n_0 = 1 \times 10^{12} \text{ cm}^{-3}$, $H_0 = 1.2 \text{ kOe}$, air at $P_0 = 8 \times 10^{-5} \text{ mm Hg}$.

if the effective velocity of the current-carrying electrons $v_{\text{cur}} > \sqrt{2kT_e/M}$ the ion-acoustic instability can be excited; when $v_{\text{cur}} > \sqrt{2kT_e/m}$ the current or "Buneman" instability can be excited; however, if the current is associated with a small fraction of the electrons then the two-stream instability can be excited, in which case we require $v_{\text{beam}} > \sqrt{2kT_e/m}$, that is to say, a velocity higher than the electron thermal velocity.

The experimental results given above show that the strongest instability develops in certain well-defined regions of the current-carrying plasma. It may be assumed that as a consequence of the axial inhomogeneity of the initial electron density (especially in the electrode regions) any of the instabilities indicated above should be concentrated in this region. The excitation of large amplitude oscillations leads to the appearance of an anomalous resistance, an increase in the real voltage, and a strong localization of the plasma heating. Evidently under these conditions a succession of all three stages of the current instability is possible. This feature is indicated to some degree by measurements of the electron energy distribution for electrons that arrive at the anode in the turbulent regime. These measurements show that whereas up to the beginning of the current break the electron energy distribution is approximately Maxwellian, at the break the electron spectrum is more like that of a relaxing beam, in which the density of electrons arriving at the anode under these conditions is generally much smaller than the plasma density. However, since we have not yet carried out measurements of the degree of randomness of the low-frequency and high-frequency oscillations, it is still difficult to suggest any actual mechanism for the heating. Nonetheless it is reasonable to point out the following situation: in the initial stage of current flow in operation with heavy gases (air, krypton) the condition for excitation of the ion-acoustic instability is satisfied in these experiments at a current density of approximately 10 A/cm^2 ; however, if this instability appears in any way its effect on the resistance of the gap and the volt-ampere characteristics is insignificant compared with the conditions that obtain when $\eta > 1$. We also note that the frequency of the low frequency oscillations exceeds the value ω_{01} .

The development of turbulence described above does not necessarily depend on the presence of electrodes. Thus, the explanation of observed effects of turbulence and anomalous heating in toroidal systems^[14,15] in terms of predictions of the theory of the two-stream or ion-acoustic instability can be established more strongly after careful measurements of the potential distribution over the length of the plasma.

An analysis of the experiments that have been carried out to investigate the mechanisms involved in exploding wires^[16] indicate a great deal of similarity between the effects observed there and effects in the present work. The current density is approximately 10^8 A/cm^2 , in which case one observes effects that accompany the appearance of a current break, and anomalous increase in the resistance and a second ignition of the discharge gap; this current density can satisfy the requirement $v_{\text{cur}} > \sqrt{2kT_e/M}$, which is necessary for the ion-acoustic instability. These results are supported by other information concerning the apparent structure of the exploding wire at this point at the stage of the cur-

rent break.^[16] The alternation of gaps of metal and the evaporating metallic plasma and vapors are actually a model for a pulsed x-ray tube^[17] which, in turn, appears as nothing more than a prototype for a turbulent straight discharge with preliminary ionization. The volt-ampere characteristics of such tubes have been studied in detail and at the present time there are clear indications that these tubes exhibit effects due to collective plasma properties.

In the present work we have not dealt with the question of determining the exact energy balance and the heating efficiency. However, under optimum conditions, even in the first half-cycle of the current we find an absorption of 50 to 80% of the energy stored in the capacitor bank. The energy evolved in the plasma in the form of thermal motion of the particles amounts to several percent. Preliminary experiments carried out with conventional calorimeters have shown that the predominant fraction of the energy evolves at the anode of the discharge. Because of the fact that $v_a \sim v_{Te}$ in the turbulent regime it is reasonable to assume that for the conditions of the present experiments the ratio of the electron kinetic energy at the anode to the total stored energy is approximately unity.

The authors wish to thank Academician R. Z. Sagdeev, Yu. E. Nesterikhin and D. D. Ryutov for their interest in the present work and S. M. Turkin and V. A. Rastoropov for help in carrying out the experiments.

¹M. V. Babykin, P. P. Gavrin, E. K. Zavoiskii, L. I. Rudakov, and V. A. Skoryupin, *Zh. Eksp. Teor. Fiz.* **47**, 1597 (1964) [*Sov. Phys. JETP* **20**, 1073 (1965)].

²M. V. Babykin, P. P. Gavrin, E. K. Zavoiskii, S. L. Nedoseev, L. I. Rudakov, and V. A. Skoryupin, *Zh. Eksp. Teor. Fiz.* **52**, 643 (1967) [*Sov. Phys. JETP* **25**, 421 (1967)].

³V. A. Suprunenko, Ya. B. Faĭnberg, V. T. Tolok, E. A. Sukhomlin, N. I. Reva, P. Ya. Burchenko, E. D. Volokov, and R. I. Rudnev, *Atomnaya ėnergiya (Atomic Energy)* **14**, 349 (1963).

⁴V. A. Simonov, V. V. Abozovik, and V. V. Ignat'ev, 2-nd International Conference on Plasma Physics and Controlled Nuclear Fusion Research, Culham, CN 21/167, IAEA, 1966.

⁵A. I. Karchevskii, A. P. Babichev, Yu. A. Muromkin, and E. M. Buryak, *Zh. Eksp. Teor. Fiz.* **53**, 3 (1967) [*Sov. Phys. JETP* **26**, 1 (1968)].

⁶L. V. Dubovoĭ and V. P. Fedyakov, *Dokl. Akad. Nauk SSSR* **167**, 553 (1966) [*Sov. Phys.-Doklady* **11**, 239 (1966)].

⁷E. K. Zavoiskii, S. L. Nedoseev, and L. I. Rudakov, *ZhETF Pis. Red.* **6**, 951 (1967) [*JETP Lett.* **6**, 367 (1967)].

⁸T. H. Jensen and F. R. Scott, *Phys. Rev. Letters* **19**, 1100 (1966).

⁹R. Z. Sagdeev, *Reviews of Plasma Physics, Consultants Bureau, New York, 1966, Vol. 4.*

¹⁰L. I. Rudakov and L. V. Korablev, *Zh. Eksp. Teor. Fiz.* **50**, 220 (1966) [*Sov. Phys. JETP* **23**, 145 (1966)].

¹¹L. V. Dubovoĭ, A. G. Ponomarenko, and O. M. Shvets, *Voprosy magnitnoĭ gidrodinamiki plazmy (Problems in Plasma Magnetohydrodynamics)* Atomizdat, 1962 Vol. 2, p. 201.

¹²L. V. Dubovoĭ, V. A. Kornilov, and A. G. Ponomarenko, Trudov Mezhvuzovskoĭ konferentsii po novoĭ tekhnike (Proc. of Interschool Conference on New Technical Methods), 1962.

¹³D. N. Lin and V. A. Skoryupin, Zh. Eksp. Teor. Fiz. **53**, 463 (1967) [Sov. Phys. JETP **26**, 305 (1968)].

¹⁴S. D. Fanchenko, B. A. Demidov, N. I. Elagin, and D. D. Ryutob, Zh. Eksp. Teor. Fiz. **46**, 497 (1964) [Sov. Phys. JETP **19**, 337 (1964)].

¹⁵S. M. Hamberger, A. Melein, J. H. Adlam, and M. Friedman, Phys. Rev. Letters **19**, 350 (1967).

¹⁶F. Webb, H. Hilton, P. Levin, and E. Tollestrup, in: Exploding Wires, Plenum Press, 1962.

¹⁷S. K. Handel and I. Sundstrom, Z. Physik **188**, 506 (1965).

Translated by H. Lashinsky
167